Plant Mol Biol (2006) 62:897–912
DOI 10.1007/s11103-006-9064-4

Characterization of the plant Notchless homolog, a WD repeat protein involved in seed development

Sier-Ching Chantha · B. Starling Emerald · Daniel P. Matton

Received: 9 May 2006 / Accepted: 23 July 2006 / Published online: 28 September 2006

Abstract We have isolated a plant *NOTCHLESS* (*NLE*) homolog from the wild potato species *Solanum chacoense* Bitt., encoding a WD-repeat containing protein initially characterized as a negative regulator of the Notch receptor in animals. Although no Notch signaling pathway exists in plants, the *NLE* gene is conserved in animals, plants, and yeast. Overexpression of the plant *ScNLE* gene in *Drosophila* similarly affected bristle formation when compared to the overexpression of the endogenous *Drosophila NLE* gene, suggesting functional conservation. Expression analyses showed that the *ScNLE* gene was fertilization-induced and primarily expressed in ovules after fertilization, mainly in the integumentary tapetum (endothelium). Significant expression was also detected in the shoot apex. Promoter deletion analysis revealed that the *ScNLE* promoter had a complex modulatory architecture with both positive, negative, and tissue specific regulatory elements. Transgenic plants with reduced levels of *ScNLE* transcripts displayed pleitotropic phenotypes including a severe reduction in seed set, consistent with *ScNLE* gene expression pattern.

S.-C. Chantha · D. P. Matton (✉)
Institut de Recherche en Biologie Végétale (IRBV), Département de sciences biologiques, Université de Montréal, 4101 rue Sherbrooke est, H1X 2B2 Montréal, QC, Canada
e-mail: dp.matton@umontreal.ca

B. S. Emerald
The Liggins Institute, Faculty of Medical and Health Sciences, The University of Auckland, Private Bag 92019, Auckland, New Zealand

Keywords Notchless · WD-repeat protein · Fertilization · Ovule · Seed

Abbreviations
DAP Days after pollination
HAP Hours after pollination

Introduction

In the life cycle of a flowering plant (angiosperm), a new sporophytic generation is established during seed development. Seed development is initiated by double-fertilization of the egg-cell and central cell of the female gametophyte, which is embedded within the maternal sporophytic integument(s) of the ovule, by the two sperm cells of the pollen. Double-fertilization triggers several developmental programs, mainly: the fertilized egg-cell initiates embryogenesis, the fertilized central cell forms a triploid nucleus that divides to give rise to the endosperm, and the integument starts differentiating into the seed coat. In coordination with seed development, the ovary develops into a fruit (Gillaspy et al. 1993). The molecular mechanisms underlying fertilization and initiation of seed development events, such as pollen tube guidance, pollen tube reception, and interactions between the different seed components (embryo, endosperm, ovule integument), likely involves intercellular signaling (Chaudhury et al. 1997; Huck et al. 2003; Marton et al. 2005; Ohad et al. 1996; Rotman et al. 2003). In animals, numerous cell fate decisions and developmental

processes rely on cellular signaling through the Notch pathway. Determining whether initially equivalent cells will adopt epidermal or neural identity in *Drosophila* and controlling germline proliferation in *C. elegans* represent only few examples (reviewed in Artavanis-Tsakonas et al. 1999; Kimble and Simpson 1997). The Notch pathway occurs between adjacent signaling cell (ligand-expressing) and receiving cell (receptor-expressing). The skeleton of this pathway is made of three conserved core components: a transmembrane DSL (Delta, Serrate, Lag-2) ligand, a transmembrane Notch-type receptor, and a downstream CSL (CBF-1, Su(H), Lag-1) transcriptional effector. The DSL ligand extracellular domain of a signaling cell first interacts with the Notch-type extracellular domain of a receiving cell. This interaction leads to the activation of the Notch intracellular domain (NICD) by releasing it from the plasma membrane. The NICD is then translocated into the nucleus where it serves as a coactivator of a CSL transcription factor to modulate gene expression. The receiving cell thus acquires an identity that differs from its adjacent signaling cell.

Several proteins are known to be positive or negative regulators of the Notch signaling activity (reviewed in Kadesch 2000). Among these, the *Drosophila melanogaster* NOTCHLESS (DmNLE) protein was shown to be a modifier of Notch activity by genetic studies and to interact with the intracellular domain of Notch by GST pull-down and immunoprecipitation assays (Royet et al. 1998). Some mutant alleles of the *Drosophila* Notch receptor (called *notchoid*) cause the formation of notches on the edge of the fly's wings. The *DmNLE* gene was isolated in a genetic screen as a dominant mutant that could suppress this notching, explaining the origin of its name. How DmNLE regulates Notch signaling activity remains however unclear. Interestingly, the mouse *NLE* homolog was found as a candidate gene for a maternal factor present in oocytes that causes the DDK syndrome, which is defined by embryonic lethality of embryos from crosses between DDK females and non-DDK males (Le Bras et al. 2002).

The *NLE* gene encodes a WD-repeat (WDR) protein. The main feature of WDR proteins is the WD motif, which is almost exclusively found in eukaryotes. This motif is defined as a stretch of 44–60 amino acids usually containing a Trp-Asp (WD) dipeptide at its C-terminus and a Gly-His (GH) dipeptide 11–24 residues downstream from its N-terminus, but exhibiting only a limited amino acid sequence conservations at each other individual position (Smith et al. 1999; Yu et al. 2000). The WD motifs are repeated in tandem from 4 to 16 times within a polypeptide and fold together into a propeller-shape platform that serves in coordinating simultaneous and/or sequential protein–protein interactions with multiple partners (Smith et al. 1999). Despite being structurally related, members of the WDR protein superfamily are however functionally very diverse. They are in fact involved in a vast array of molecular mechanisms such as signal transduction, RNA processing, cytoskeletal dynamics, chromatin modification, and transcriptional mechanisms, to name a few examples (reviewed in Neer et al. 1994; van Nocker and Ludwig 2003).

In *Arabidopsis*, van Nocker and Ludwig (2003) identified 237 WDR proteins and classified them into 143 distinct families according to sequence similarities. Among these, some well characterized WDR proteins were shown to regulate various development processes in plants. For example, FIE and MSI1 are two WDR proteins that together associate with MEA in a higher protein complex to repress gene transcription in the central cell of the embryo sac (Kohler et al. 2003). Their activity is required to repress the initiation of endosperm development in the absence of fertilization. Loss-of-function mutations in these genes lead to precocious endosperm formation without the need for fertilization (Chaudhury et al. 1997; Kohler et al. 2003; Ohad et al. 1996). *Msi1* mutants also initiate parthenogenetic development of the embryo (Guitton and Berger 2005). Also involved in embryo and seedling development, mutations in the TANMEI/EMB2757 WDR protein have recently been shown to produce pleiotropic phenotypes (Yamagishi et al. 2005). LEUNIG is another WDR protein reported to function as a putative transcriptional co-repressor in the regulation of the *AGAMOUS* floral homeotic gene expression (Conner and Liu 2000). One more example is COP1, a protein that possesses in addition a RING-finger motif and is proposed to act as an E3 ubiquitin ligase in the ubiquitin-proteasome degradation pathway (Osterlund et al. 2000). Because *cop1* mutants show a photomorphogenic development when grown in the dark, COP1 is defined as a negative regulator of photomorphogenic development in the dark (Deng et al. 1991). Other WDR proteins are involved in cell cycle regulation, such as CCS52, a mitotic inhibitor that is required for endoreduplication (Cebolla et al. 1999). These few examples demonstrate the importance of WDR proteins in the regulation of diverse aspects of plant development.

In this report we describe the characterization of a plant homolog of the *DmNLE* gene in *Solanum chacoense* (*ScNLE*). Based on the analysis of the *Arabidopsis* genome, most of the known components

of the Notch signaling pathway are absent from plants (Wigge and Weigel 2001). However, overexpression experiments of the plant *Nle* homolog in *Drosophila* showed that ScNLE retains the capability to interact with the Notch receptor. In *S. chacoense*, *ScNLE* expression is associated to the shoot apex and is also transiently induced by fertilization in the endothelium of ovules. Analysis of transgenic plants underexpressing *ScNLE* suggests a specific role in fertilization and/or post-fertilization events for this gene as well as a more general role in shoot development.

Material and methods

Plant material and growth conditions

The diploid ($2n = 2x = 24$) *Solanum chacoense* Bitt. (Potato Introduction Station, Sturgeon Bay, WI) self-incompatible genotypes include line G4 (S_{12} and S_{14} self-incompatibility alleles) as female progenitor and line V22 (S_{11} and S_{13} alleles) as pollen donor. Plants were maintained by in vitro propagation on ½MS medium with charcoal (0.5× MS salts, 1× MS vitamins, 20% sucrose, 0.5% deactivated charcoal, 0.6% agar, pH 5.8) at 20–22°C with a photoperiod of 16 h light and 8 h dark. Plants from 1 to 2 months old were transferred to soil and were grown in a greenhouse with an average of 14 h of light/day for flower and fruit development analyses.

Library construction and virtual subtraction

The cDNA library was made from 5 μg of poly(A)$^+$ mRNA isolated from pistils 48 HAP in the ZAP express pBK vector (Stratagene, LaJolla, CA) (Lantin et al. 1999). In order to enrich the screened library for non-redundant and weakly expressed transcripts, a negative selection screen was performed (Germain et al. 2005).

Isolation and gel blot analysis of RNA and DNA

Isolation and gel blot analyses of RNA and DNA were performed as described previously (Lagacé et al. 2003; Lantin et al. 1999). Membranes were exposed at –85°C with intensifying screens on Kodak Biomax MR film (Interscience, Markham, ON).

In situ hybridization

In situ detection of *ScNLE* was performed as described previously (Lantin et al. 1999). Sense and antisense digoxigenin-11-UTP (Roche Diagnostics, Laval, QC) labeled riboprobes were synthesized from the *ScNLE* cDNA cloned in the pBK vector using T3 and T7 RNA polymerases (RNA transcription kit, Stratagene) after linearization of the plasmid with *Xho*I or *Eco*RI, respectively.

ScNLE constructs for underexpression

For gene suppression using the antisense strategy, a ~1500 bp fragment of *ScNLE* cDNA was cloned in the antisense orientation in the pBIN35S double-enhancer vector (Bussiere et al. 2003). For gene suppression using the double-stranded RNA interference strategy, a ~650 bp fragment of *ScNLE* cDNA was cloned in the sense and antisense orientations in the pDarth vector (O'Brien et al. 2002) from PCR products obtained with the NLE14 (5′-GAGA**GGATCC**AAACCACGCAGGGGAAGCTA-3′) and NLE18 (5′-GAGAGGCGC**GGTACC**CTATCCCATCCATAGCTTCAG-3′) primers containing the *Bam*HI and *Xho*I restriction sites, respectively, and with the NLE19 (5′-GAGA-**CTCGAG**AAACCACGCAGGGGAAGCTA-3′) and NLE22 (5′-GAGA**GGCGCGCC**CTATCCCATCCATAGCTTCAG-3′) primers containing the *Xho*I and *Asc*I restriction sites, respectively. Plant transformation with *Agrobacterium tumefaciens* strain LBA4404 was carried out as described previously (Matton et al. 1997).

Semi-quantitative RT-PCR

RNA samples were purified from DNA contamination by treatment with Rnase-free Dnase I on Rneasy® colums (Qiagen, Mississauga, ON), according to the manufacturer's instructions. RNA samples were reverse transcribed by using the M-MLV reverse transcriptase (Invitrogen Canada, Burlington, ON), according to the manufacturer's instructions, using 0.1 μg/μl oligo dT_{20}, 2 U/μl RNaseOUT (Invitrogen Canada), and 0.1 μg/μl total RNA. PCR mixtures contained 1/20 vol of cDNA sample, 1 μM forward and reverse primers, 200 μM dNTP, 1× *Taq* buffer and 0.025 U/μl HotStartTaq DNA polymerase (Qiagen). Endogenous *ScNLE* was amplified with the NLE20 (5′-GAGAGGTACCCCTCTATTTCCTCTTAAGAG-3′) and NLE3 (5′-TAGCGTTTTCAGGGAGGTAC-3′) primers and *ACTIN* was amplified with the Act-1F (5′-CTGARGCMCCYCTTAAYCCCAAG-3′) and Act-1R (5′-GTGRCTSACACCATCACCAGAGT-3′) degenerated primers. PCR reactions were performed under the following conditions: 1 cycle of 95°C/15 min; varying number of cycles of 94°C/30 s, 57°C/30 s, 72°C/30 s; 1 cycle of 72°C/5 min.

ScNLE promoter cloning

A genome walking technique was used to isolate the promoter of the *ScNLE* gene. Genomic DNA of *S. chacoense* was isolated with the DNeasy Plant Mini Kit (Qiagen). Adaptor-ligated genomic DNA libraries construction and PCR-based DNA walking were performed according to a modified protocol of the Universal GenomeWalker Kit (Clontech). Three microgram of genomic DNA aliquots were separately digested with *Dra*I, *Eco*RV, *Nae*I, *Pvu*II, *Stu*I, and *Sma*I restriction enzymes. Blunt-ended DNA fragments were then ligated to the GenomeWalker adaptors. Primary PCR amplifications were performed with adaptor-specific AP1 and gene-specific NLE26 (5′-TTGCCTTCTGGGTCTGCCAACTGACATATG-3′) primers and r*Tth* DNA Polymerase (Perkin Elmer) using a manual hot start (40 µl PCR mix: 1 µl DNA library; 21.68 µl deionized H_2O; 1× XL buffer II; 0.2 mM dNTP mix; 1.1 mM $Mg(OAc)_2$; 0.1 µM AP1 primer; 0.1 µM NLE26 primer. 10 µl hot start mix: 5.97 µl deionized H_2O; 1× XL buffer II; 2 U r*Tth* DNA Polymerase). PCR program: 96°C, 5 min; 7 cycles—94°C, 25 s, 72°C, 3 min; 32 cycles—94°C, 25 s, 67°C, 3 min; 67°C, 7 min. Secondary PCR amplifications were performed with nested adaptor-specific AP2 and gene-specific NLE27 (5′-AGCTTCCACTTC-CACTTCCATCGTTTCTGC-3′) primers (40 µl PCR mix: 1 µl primary PCR product; 21.68 µl deionized H_2O; 1× XL buffer II; 0.2 mM dNTP mix; 1.1 mM $Mg(OAc)_2$; 0.1 µM AP2 primer; 0.1 µM NLE27 primer, 10 µl hot start mix: 5.97 µl deionized H_2O; 1× XL buffer II ; 2 U r*Tth* DNA Polymerase). PCR program: 94°C, 5 min; 5 cycles—94°C, 25 s, 72°C, 3 min; 20 cycles—94°C, 25 s, 67°C, 3 min; 67°C, 7 min. DNA fragments obtained from secondary PCR were gel-extracted with the QIAquick Gel Extraction kit (Qiagen) and cloned with the TOPO TA cloning system according to the manufacturer's instructions (Invitrogen). Cloned DNA fragments were sequenced to confirm identity.

Promoter–GUS fusion constructs

Four regions of the *ScNLE* promoter were PCR amplified from *S. chacoense* genomic DNA using PWO DNA Polymerase (Roche Diagnostics, Laval, Qc). The vector pCambia-1291Z (CAMBIA, Canberra, Australia) was used to create translational fusions with the GUS reporter gene. The upstream primers used for amplifying promoter DNA fragments of various sizes were: NLE31 (–1171) 5′-GAGAGAATTCTTGGA-GCGTGTTTTATCAAG-3′; NLE30 (–695) 5′-GA-GAGAATTCAGCTATATTAGCTCACCGTTC-3′; NLE29 (–400) 5′-GAGAGAATTCTGCCAAATGT-GAAACAATGTC-3′; and NLE36 (–113) 5′-GAG-AGAATTCATCTTTGCAAAGCTGAAA-3′. These upstream primers were tagged with the *Eco*RI restriction site sequence (underlined in the above mentioned primers). The downstream primer NLE28 (5′-GAGACCATGGCACTGTTTGTTGCTTCTCT-C-3′) is tagged with the *Nco*I restriction site (underlined) and was used in all the PCR amplifications. The 3′ nucleotide position for all the promoter regions cloned corresponds to +58. PCR products were digested with and ligated to the *Eco*RI and *Nco*I sites of pCambia1291Z. The amplified sequences and junctions of the construct were confirmed by sequencing. Plant transformation with *Agrobacterium tumefaciens* strain LBA4404 was carried out as described previously (Matton et al. 1997).

GUS staining

Tissues were collected and immediately fixed in 90% ice-cold acetone and incubated 20 min at room temperature. Tissues were rinsed twice with a GUS working solution (50 mM sodium phosphate, pH 7.2, 2 mM $K_3Fe(CN)_6$, 2 mM $K_4Fe(CN)_6$, and 0.2% Triton X-100) for 20 min each at room temperature. After rinsing, tissues were vacuum infiltrated for 40 min with 5-bromo-4-chloro-3-indolyl β-D-glucuronide cyclohexylamine (X-Gluc) salt, added to GUS working solution to a final concentration of 2 mM, and then incubated at 37°C overnight. The reaction was terminated and tissues were cleared in 70% ethanol added fresh once a day for a week.

Microscopy

Plant material embedded in paraffin was prepared for sectioning as described for in situ hybridization. Tissues stained for GUS expression were fixed in formaldehyde-acetic acid (3.7% formaldehyde, 5% acetic acid, and 50% ethanol) for 2 h and dehydrated through an ethanol series and embedded in paraffin. Paraffin blocks were trimmed to reveal internal tissues and surface-exposed tissues were counter-stained with safranin to localize GUS coloration (Kim et al. 2002). Sectioned tissues were visualized under a dissecting microscope. For flower buds morphology analysis, sections 10 µm thick were rehydrated and stained with safranine overnight, thoroughly washed in water and then stained with Astra blue for 20 min. After two washes in water, sections were dehydrated and mounted in Permount.

DNA analysis

Database searches were conducted with the BLAST program at The Arabidopsis Information Resource (www.arabidopsis.org) and at the National Center for Biotechnology Information (www.ncbi.nlm.nih.gov).

Drosophila transformation

Details on overexpression experiments in *Drosophila* have been described previously (Royet et al. 1998).

Results

Isolation of the *NLE* gene in *Solanum chacoense*

Key regulatory genes involved in development, as opposed to housekeeping genes, are generally weakly expressed and highly tissue-specific (Hu et al. 2003). We have initiated a negative selection screen targeting weakly expressed genes, with the aim of identifying regulatory genes involved in fertilization and seed initiation in *Solanum chacoense* (a close relative of the potato and tomato) (Germain et al. 2005). *S. chacoense* is self-incompatible and pollination time can therefore be easily controlled. Pollen tubes reach the first ovules in the ovary around 36 h after pollination (HAP) and fertilization is completed for all ovules around 42–48 HAP (Clarke 1940; Williams 1955 and our unpublished observations). The selection screen was initially carried on 2000 clones obtained from a cDNA library of pistils collected 48 HAP. A total of 250 clones were selected and sequenced. A homolog of the *Drosophila melanogaster NLE* gene (*DmNLE*) was isolated and named *ScNLE* (for *Solanum chacoense NLE*). The *DmNLE* gene was initially isolated in a suppressor screen in a viable Notch receptor mutant background and was characterized as a regulator of Notch signaling activity (Royet et al. 1998).

The longest *ScNLE* cDNA isolated consisted of 1,827 bp (excluding the poly A tail) and likely represented the full-length or near full-length *ScNLE* mRNA since it corresponded to the size of the mRNA detected in gel blot analyses (~1.8 kb). The *ScNLE* cDNA contained a single long open reading frame (ORF) with two in frame initiation codons at positions 65 (AGAUUAAUGGCA) and 77 (AAACGAUGGAA) from the first nucleotide of the cDNA. The second AUG thus shows higher similarity with the plant translation start site consensus sequence for the dicots (aaA(A/C)aAUGGCu) (Joshi et al. 1997). Furthermore, sequence comparison with amino acid sequences from plant NLE orthologs (data not shown) suggests that the second ATG represents the most probable translational initiation start site. Thus, the deduced ScNLE protein is 482 aa long and has a predicted molecular weight of 53.2 kDa.

ScNLE gene copy number was determined by DNA gel blot analysis (Fig. 1B). Three hybridizing fragments could be detected from *Hin*dIII (4.5, 2.0, and 1.3 kb), two from *Eco*RV (7.0 kb and 3.0 kb), and two from *Eco*RI (5.0 kb and 4.2 kb) restriction enzymes. Since there are two *Hin*dIII (positions 233 and 1,799) and one *Eco*RV (position 1,393) sites in the cDNA sequence, this suggests that *ScNLE* is a single copy gene in *S. chacoense*. Accordingly, analysis of the *Arabidopsis* genome sequence revealed the presence of only one copy of the *AtNLE* gene (At5g52820).

Sequence analysis of ScNLE protein

A BLAST search of the GenBank protein database revealed that ScNLE exhibits highest overall similarities with plant sequences obtained from *Arabidopsis thaliana* (76% identity, 88% similarity; BAB10430) and *Oryza sativa* (78% identity, 89% similarity; ABA94577). Moreover, ScNLE showed high overall sequence conservation with orthologs from *Xenopus laevis* (56% identity, 74% similarity; AAC62236), *Saccharomyces cerevisiae* (47% identity, 68% similarity; NP_009997 or Ycr072cp) and *Drosophila melanogaster* (52% identity, 71% similarity; AAF51479).

The NLE protein contains a Nle domain followed by a WD-repeat (WDR) domain (Fig. 1A). The Nle domain was defined as a region with a high degree of sequence conservation in the N-terminal portion of NLE homologs (Royet et al. 1998). *S. chacoense* and *D. melanogaster* Nle domains are 42% identical (64% similar). Use of predictive tools (http://BMERC-www.bu.edu/wdrepeat) allowed the identification of eight WD repeats in the WDR domain of ScNLE (Fig. 1A). A WD motif is defined as a stretch of 44–60 aa that typically contains the GH dipeptide 11–24 residues from its N-terminus and the WD dipeptide at its C-terminus, but that exhibits only a limited amino acid sequence conservation at each individual position (Smith et al. 1999; Yu et al. 2000). Seven of the eight WD repeats in ScNLE range from 41 to 48 aa in length. The fifth WD motif is unusually long (78 aa) and Royet et al. (1998) considered this fifth repeat as representing two different WD repeats lacking the signature residues. Our analyses indicated instead that this region represents a unique WD repeat that contains a small insertion. Surface-exposed residues in a WD repeat are predicted to be grouped in the variable regions I and II

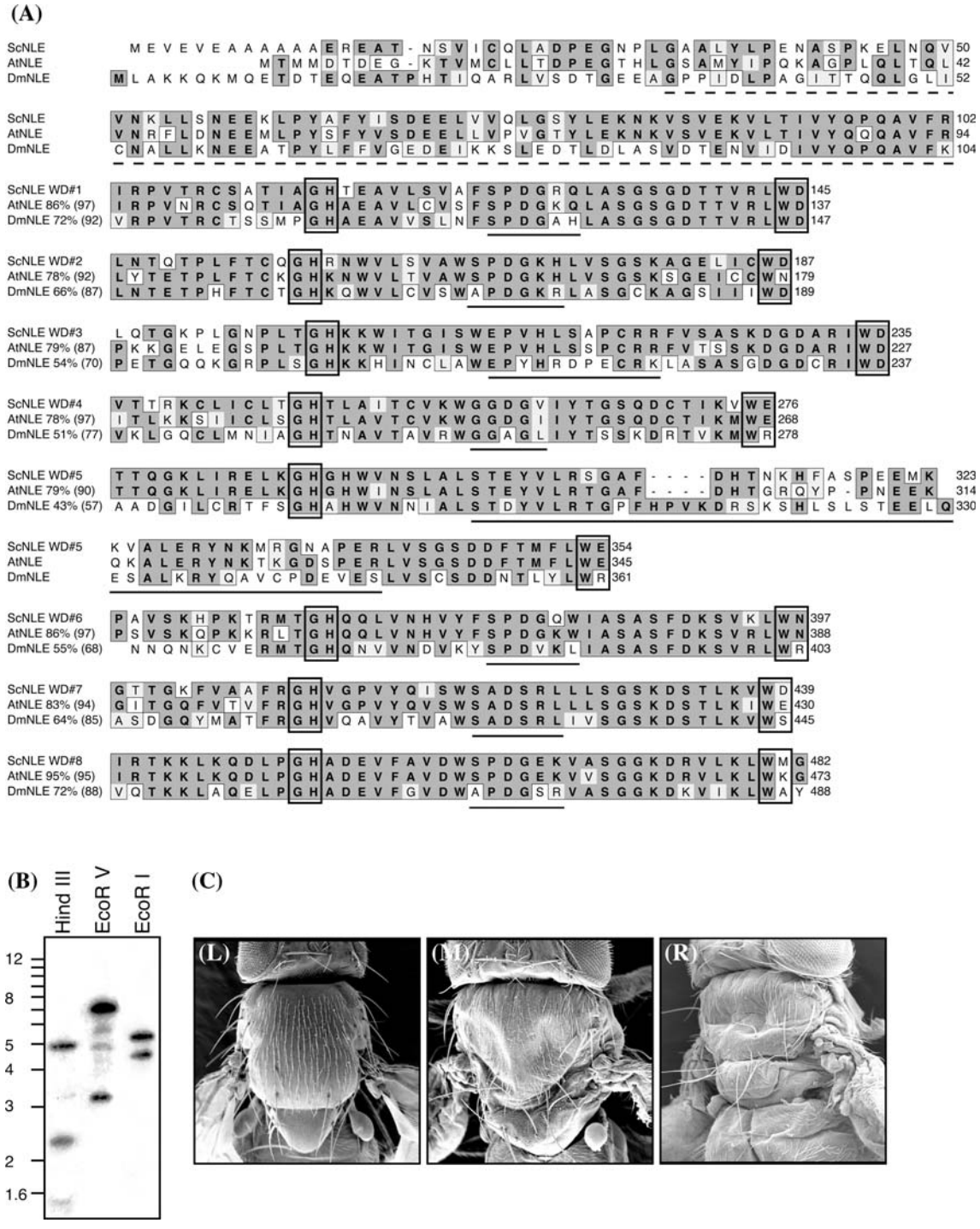

Fig. 1 (**A**) Alignment of ScNLE, AtNLE, and DmNLE amino acid sequences. The NLE domain is indicated with a dashed line. The eight WD motifs that constitute the WDR domain are numbered on the left with percentage of sequence identity and similarity (in parenthesis) compared to ScNLE. The conserved dipeptides GH and WD of each WD motif are boxed. The variable regions I comprise the amino acids preceding the GH of each WD motif. The variable regions II are underlined. Sequence identity is highlighted in dark gray and similarity in light gray. Dashes indicate gaps introduced to maximize homology. (**B**) DNA gel bot analysis of the *ScNLE* gene. Genomic DNA (10 μg) was digested with the restriction enzymes indicated on top and probed with the complete 1.8 kb ^{32}P-labeled *ScNLE* cDNA. Molecular weight markers are indicated in kb on the left. (**C**) Effects of overexpression of *ScNLE* on thoracic bristle formation in *Drosophila*. SEM images of the thorax of an ApGal4/+ line (left); a weak overexpressing *ScNLE* line ApGal4/UAS-ScNLE (middle); and a strong overexpressing *ScNLE* line ApGal4/UAS-ScNLE (right)

(Smith et al. 1999) (Fig. 1A). These regions are responsible for most protein variability and would determine the specificity of protein interaction with protein partners. Despite a high overall homology between corresponding WD repeats of ScNLE and DmNLE, ranging from 43% to 72% identity, comparison of their corresponding variable regions I and II revealed a variation in the degree of sequence identity, with very low conservation found in some of these regions. On the basis of these observations, some protein partners of ScNLE and DmNLE have likely diverged in plant and animal organisms.

ScNLE is a partial functional homolog of DmNLE in *Drosophila*

To determine whether the high overall amino acid sequence identity between ScNLE and DmNLE reflects conservation in protein function, the plant *ScNLE* gene was overexpressed in the thorax of fruit flies by driving a UAS::ScNLE construct under the control of apterous::GAL4 (apGAL4). In *Drosophila*, modulating the Notch signaling pathway influences, among other things, the number of thoracic cells that differentiate into bristle instead of epidermal cell. The overexpression of *DmNLE* in *Drosophila* was reported to cause a significant reduction in the number of bristles formed on the thorax (196.0 ± 3.0, $n = 17$) compared to apGAL4 control lines (214.2 ± 2.7, $n = 9$) (Royet et al. 1998). Interestingly, the overexpression of *ScNLE* also caused a significant reduction in the number of thoracic bristles formed, with an average of 187.9 ± 8.1 bristles per thorax ($n = 16$, $P < 0.001$) (Fig. 1C). This result indicates that ScNLE is able to accomplish, at least partially, the same function as DmNLE protein when overexpressed in flies. However, some strong *ScNLE* overexpressing lines obtained from these experiments were associated with phenotypes never observed in *DmNLE* overexpressing lines. Strong *ScNLE* overexpressing lines produced much less bristles comprising large, medium, and also unusual tiny bristles (Fig. 1C). Furthermore, the fly's thorax seemed to collapse, suggesting the loss of some internal tissues. Since these additional phenotypes were not observed with *DmNLE* overexpression, it is likely that ScNLE and DmNLE are not fully functional homologous proteins, as can be expected.

ScNLE expression pattern in *Solanum chacoense*

ScNLE mRNAs expression pattern was determined in plant tissues by RNA gel blot analyses. We first focused on *ScNLE* expression pattern in ovaries since *ScNLE* cDNA was isolated from a pollinated pistil cDNA library. Figure 2A shows a broad time-course analysis using isolated ovules. Weak expression signal was detected in ovules from unpollinated flowers (0 h). Interestingly, the expression was strongly and transiently increased 2 days after pollination (DAP), decreasing to basal levels by 4 DAP. A more detailed time-course analysis was also carried out with pollinated ovaries (Fig. 2B). *ScNLE* expression was weak from 0 h to 30 h after pollination (HAP) and was significantly increased at 36 HAP. Peak expression was reached around 42 HAP (Fig. 2B) and then slowly declined to basal levels (Fig. 2A). This transient increase in *ScNLE* gene expression around 36–42 HAP corresponds exactly to the intense period of basipetal fertilization of the multiple ovules present in the ovary and to the initiation of seed development in some Solanaceous species, including *S. chacoense* (Clarke 1940; Williams 1955, and our unpublished results). To confirm that the strong increase in *ScNLE* expression

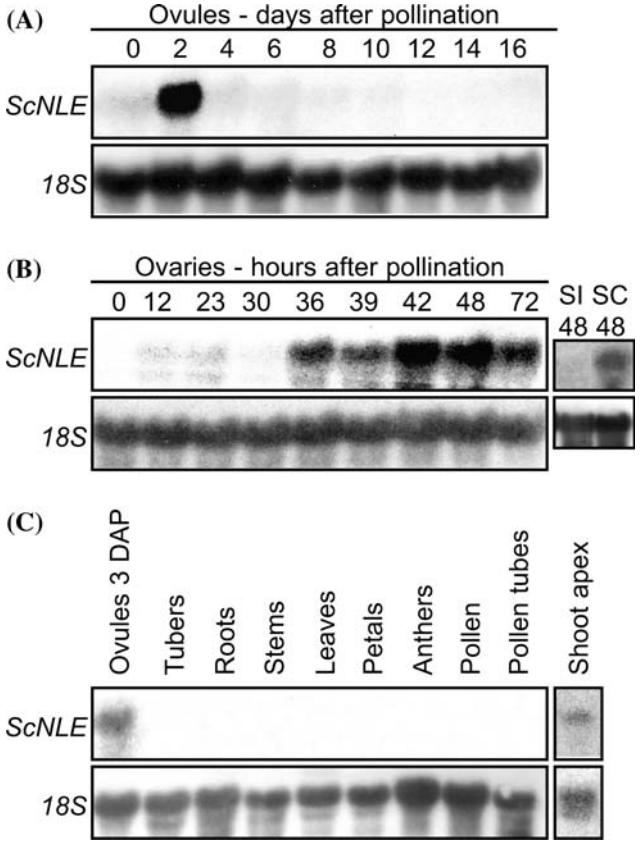

Fig. 2 RNA expression analysis of *ScNLE* transcript levels. Ten microgram of total RNA from various tissues were probed with a ^{32}P-labeled *ScNLE* cDNA. (**A**) Ovules at different time points in days after pollination (DAP). (**B**) Ovaries at different time points in hours after pollination (HAP) and comparison between a compatible (SC) and an incompatible (SI) pollination 48 HAP. (**C**) Mature plant tissues and the shoot apex

was fertilization-dependent and not only a consequence of pollination, we took advantage of the gametophytic self-incompatibility system present in *S. chacoense*. Following a self-incompatible pollination, pollen tubes are normally stopped in the top 2/3 of the style and no increase in *ScNLE* mRNA levels could be observed in ovaries (Fig. 2B). This result confirmed that the increase in *ScNLE* expression was fertilization-dependent.

We also tested for *ScNLE* expression in various plant tissues. Figure 2C shows that no signal was detected in the vegetative tissues tested, including tubers, roots, stems, and leaves, nor in floral organs such as petals, anthers, and pollen grains or tubes. RNAs from ovaries 3 DAP served as a positive control in this RNA gel blot. Although no expression could be initially detected in vegetative tissues, shoot apices containing the shoot apical meristem and organ primordia were also tested (see also transgenic phenotype section below). As for other tissues tested, a single band of ~1.8 kb, corresponding to the length of the longest *ScNLE* cDNA isolated, was also detected in the shoot apex (Fig. 2C).

In situ detection of *ScNLE*

In situ hybridization was used to further examine *ScNLE* mRNA expression pattern in ovaries 48 HAP, a time point corresponding to high *ScNLE* expression levels in RNA gel blot analysis (Fig. 2A). Hybridization signals were more strongly associated to the outermost cell layers of the placenta and to the endothelium (also called the integumentary tapetum) of ovules, which is the innermost cell layer of the integument (Solanaceous ovules are unitegmic) (Fig. 3A) as well as in the zygote (Fig. 3C). *ScNLE* expression was also detected in the vascular tissues of the receptacle and ovary (Fig. 3A) as well as of the funiculus (Fig. 3D). Uniform and weaker expression of *ScNLE* was detected in inner placenta cells (Fig. 3A). Equivalent tissues were hybridized with a *ScNLE* sense probe as negative controls and no signal could be detected in these tissues (Fig. 3B, E), confirming the specificity of the *ScNLE* hybridization pattern obtained. Such expression pattern suggests that *ScNLE* plays a role in some specific response immediately following fertilization.

Analysis of cis-regulatory regions required for expression of *ScNLE* in the ovary

As a first step in defining the cis-regulatory regions required for specific expression pattern of *ScNLE* in the ovary, a promoter deletion analysis was performed. A 1,171 bp fragment upstream of the translational initiation site (numbered as +1) was isolated by a genome walking technique. A series of 5′ deletions with end points at –1,171, –695, –400, and –113 from the translation start site, and comprising a part of the coding region (+58), were fused in-frame to the *uidA* reporter gene encoding the β-glucuronidase (GUS) protein (Fig. 4). The resulting chimeric gene constructs were subsequently transformed into WT *S. chacoense* plants. At least five stable trangenic plants of each construct were analyzed for the expression patterns of GUS activity. Variability in the patterns of GUS activity within the different lines generated from the same construct was observed, which is consistent with results obtained in other studies and could be attributed to position effects (Honma and Goto 2000; Tilly et al. 1998). A summary of the deletion constructs and the relative intensities of GUS staining observed in more than half of the samples, unless specified otherwise, is reported in Fig. 4. Typical GUS staining patterns from tissue sections are shown in Fig. 5. With construct PNLE-1171 in flowers 48 HAP, obvious GUS staining was found in a region of the receptacle below the ovary (Fig. 5A). This stained region of the receptacle comprised mainly the vascular tissues of the receptacle as suggested by a more precise localization in lightly stained samples (Fig. 5D). Staining was weak and uniform in the placenta with a darker outermost cell layer (Fig. 5B, C). Finally, in about one third of the ovaries analyzed, the funiculus of ovules was also stained (Fig. 5B, C). GUS activity was not detected, or sometimes only faintly detected, in petals and anthers (Fig. 5E), confirming results obtained by RNA gel blot analysis (Fig. 2C). The observed pattern of PNLE-1171 GUS staining recapitulated only partially the pattern of endogenous *ScNLE* transcripts revealed by in situ RNA hybridization (Fig. 3). In accordance, GUS activity was detected in the vascular tissues of the receptacle, in the placenta and the funiculus. However, the absence of GUS staining in the endothelium of ovules and in the vascular tissues of the ovary as well as the presence of GUS staining in the receptacle outside the vascular tissues differed from the *ScNLE* expression pattern determined by in situ hybridization (compare Figs. 3, 5A). Therefore, the –1,171 bp region upstream of the *ScNLE* gene contains some, but not all, of the regulatory elements necessary for normal expression pattern observed in the ovary, as determined by in situ hybridization. These results also suggest that a silencer element is required to inhibit *ScNLE* expression in the receptacle and that additional regulatory elements, either upstream of the –1,171

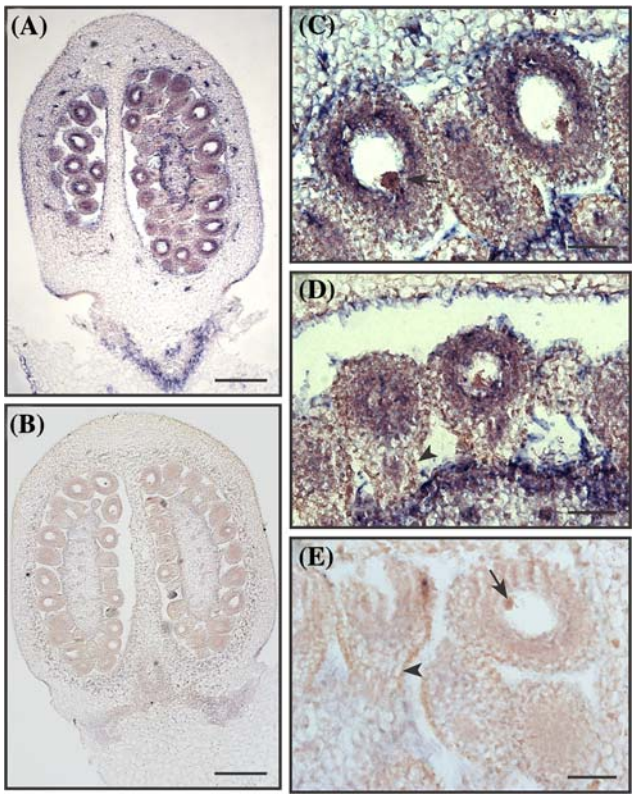

Fig. 3 In situ localization of *ScNLE* transcripts. (**A**) Ovary 48 HAP, longitudinal section, *ScNLE* antisense probe. (**B**) Ovary 48 HAP, longitudinal section, *ScNLE* sense probe. (**C**, **D**) Ovules 48 HAP, *ScNLE* antisense probe. Magnified view of portions of (**A**). Arrow indicate the zygote in (**C**) and arrowhead the funiculus in (**D**). (**E**) Ovules 48 HAP, *ScNLE* sense probe. Magnified view of portions of (**B**). Arrow indicates the zygote and arrowhead indicates the funiculus. (**A**, **B**) Bar = 250 μm. (**C**, **D**, **E**) Bar = 50 μm

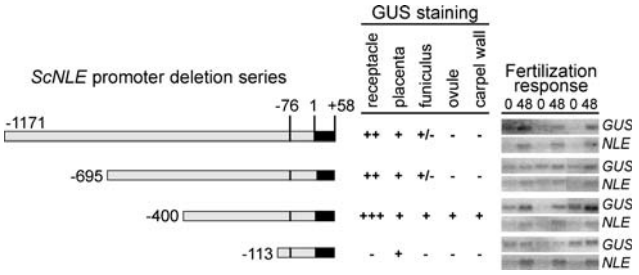

Fig. 4 *ScNLE* promoter deletion analysis. Left: Schematic representation of the *ScNLE* promoter deletion series fused to the *uidA* reporter gene. Numbers indicate nucleotide position: +1 corresponds to the first nucleotide of the ATG initiation codon, –76 represents the 5′ end of the longest *ScNLE* cDNA isolated, and numbers on the left of the schemes refer to the 5′ end nucleotide positions of the promoter regions cloned. A portion of the *ScNLE* coding region corresponding to the first 19 N-terminal amino acids (black box) has been included in the constructs to create a translational fusion with the GUS reporter gene. Middle: Summary of GUS expression patterns obtained with corresponding constructs in ovaries 48 HAP. Relative levels of GUS staining represented by: –, not detected; +, low; ++, moderate; +++, high; +/–, coloration observed in one third of the samples only. All other relative levels corresponds to observations made in more than half of the lines tested. Right: RNA gel blot analysis of regulatory regions required for *ScNLE* fertilization-induced expression using the *GUS* reporter gene as a probe and the endogenous *ScNLE* gene as an internal control

position, or downstream of the + 58 position, are also required for expression of *ScNLE* in the endothelium of ovules and vascular tissues of the placenta (Fig. 6A).

Further deletion analyses uncovered other aspects of *ScNLE* gene expression regulation. Promoter deletion up to –695 gave identical GUS staining patterns as for the PNLE-1171 construct (Fig. 5F), suggesting that the regulatory elements driving the expression pattern in the ovary 48 HAP observed with the PNLE-1171 construct are not comprised in the –1,171 to –695 region of *ScNLE* promoter. Further deletion to –400 however, led to the lost of specificity of GUS expression in the ovary (Fig. 5G). GUS distribution with the PNLE-400 construct was more extended in the receptacle and was also uniformly distributed in all the tissues of the ovary. Therefore, the –695 to –400 region of *ScNLE* promoter seems to comprise a silencer element for repression of *ScNLE* expression in several tissues of the ovary 48 HAP, such as in external regions of the receptacle, in the carpel wall, and in the ovule's integument, to allow a specific expression pattern of the gene (Fig. 6A). A further deletion to –113 abolished GUS expression in all ovary tissues 48 HAP except the placenta (Fig. 5H), suggesting that the –113 to +58 region and the –400 to –113 region contain positive regulatory elements essential for *ScNLE* expression in the placenta and the other ovary tissues, respectively (Fig. 6A).

RNA gel blot analyses showed that *ScNLE* expression in ovules and ovaries was very weak in unpollinated mature flowers (0 HAP) and was strongly increased around fertilization time (48 HAP) (Fig. 2A, B). We next wanted to determine whether a regulatory element responsible for this increase in *ScNLE* expression was present in the 1,171 bp promoter region analyzed. RNA gel blots made with total RNA extracted from ovaries at time 0 and 48 HAP after fertilization collected from the same transgenic lines used to study GUS staining patterns were probed with a labeled *GUS* insert and, as internal control, with a *ScNLE* probe to detect the expression of the endogenous *ScNLE* gene. A summary of the results is reported in Fig. 4. Equal loading of the samples was confirmed by probing with ribosomal 18S (data not shown). With construct PNLE-1171, a considerable increase in *GUS* expression levels from 0 HAP, where expression was barely detectable, to 48 HAP recapitulated the pattern of endogenous *ScNLE* expression

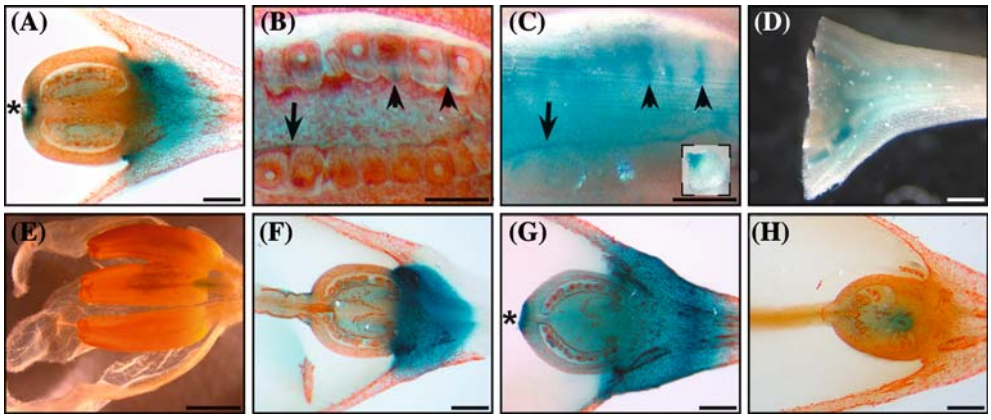

Fig. 5 GUS expression patterns in ovary and other floral organs 48 HAP conferred by 5′ deletions of the *ScNLE* promoter. (**A**) PNLE-1171, ovary 48 HAP, longitudinal section. (**B**, **C**) PNLE-1171, magnified view of a portion of (**A**) showing GUS expression in the funiculus (arrowhead) and outermost cell layer of the placenta (arrow). Bar = 200 μm. (**C**) Identical to (**B**) without safranin coloration. (**D**) PNLE-1171, whole-mount image of a lightly stained receptacle. Bar = 500 μm. (**E**) PNLE-1171, whole-mount image of anthers and petals. Bar = 2 mm. (**F**) PNLE-695, ovary 48 HAP, longitudinal section. (**G**) PNLE-400, ovary 48 HAP, longitudinal section. (**H**) PNLE-113, ovary 48 HAP, longitudinal section. (**A**, **F**, **G**, **H**) Longitudinal sections of ovaries were counter-stained with safranin (red coloration). Bar = 500 μm. (**A**, **G**) Asterisks indicate blue coloration on top of the carpel wall at the style junction observed only in a small subset of samples

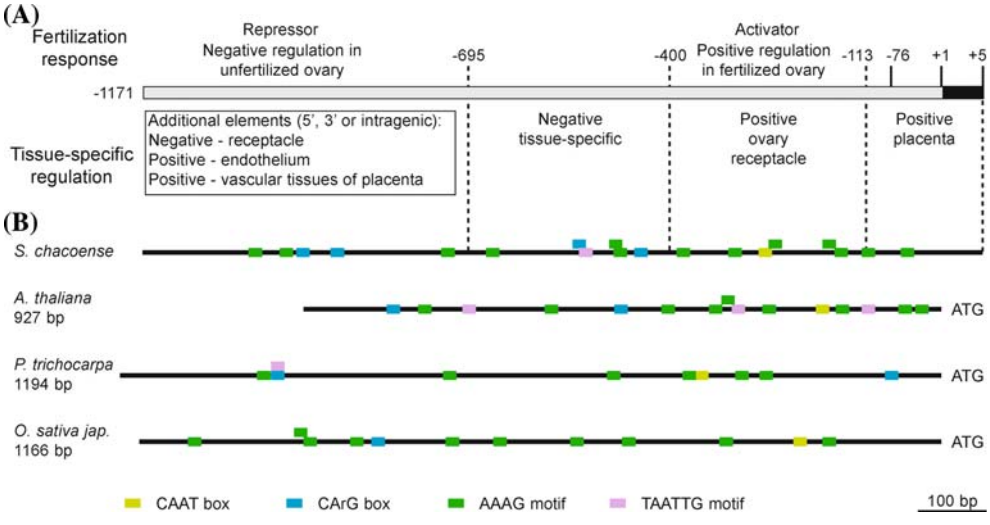

Fig. 6 Putative cis-regulatory regions and elements in the *NLE* promoter. (**A**) Summary of the regulatory regions for *ScNLE* gene expression in the ovary 48 HAP as determined by promoter deletion analysis. (**B**) Relative location of putative cis-regulatory elements in *Solanum chacoense* NLE promoter linked to the regulatory regions reported in (**A**) and also found in NLE promoters of *Arabidopsis thaliana*, *Populus trichocarpa*, and *Oryza sativa* (var. japonica)

levels, suggesting that the promoter region analyzed contained regulatory element(s) that respond to the fertilization event. Deletion of region –1,171 to –695 led to higher expression of *GUS* in ovaries 0 HAP when compared to endogenous *ScNLE* expression, suggesting that this region comprises a negative regulatory element for repression of *ScNLE* expression in the ovary in absence of fertilization (Figs. 4, 6A). Despite the appearance of *GUS* expression in ovaries 0 HAP when region –1,171 to –695 was removed, *ScNLE* promoter deletion down to –400 generally still led to an increase in *GUS* expression levels from 0 to 48 HAP. With the PNLE-695 construct in ovaries 48 HAP, *GUS* was expressed at similar levels to endogenous *ScNLE* whereas with the PNLE-400 construct, *GUS* expression was stronger than that of the endogenous *ScNLE*, a result that is consistent with loss of tissue-specific activity of *ScNLE* promoter and hence, widespread distribution of GUS, as shown previously with this construct (Figs. 4, 5G). Further promoter deletion to –113, however, completely abolished the increase in *GUS* expression levels from 0 to 48 HAP, leading to equal *GUS* expression levels at 0 and 48 HAP, lower than endogenous *ScNLE*. These results altogether suggest that region –400 to –113 of *ScNLE* promoter comprises a positive regulatory element that responds to fertilization in the ovary (Fig. 6A).

Analysis of cis-regulatory motifs in *NLE* promoter sequences

To link the cis-regulatory regions we have identified to candidate transcription factors, we searched the *ScNLE* promoter for different sequence motifs recognized by transcription factors that had been shown to be expressed in ovary tissues by in situ hybridization. Because orthologous genes frequently have common expression patterns, we also determined whether these sequence motifs were common to available putative *NLE* promoters from different plant species (*Arabidopsis thaliana*, *Oryza sativa* var. *japonica*, *Populus trichocarpa*). Regions of about the same length, upstream of the predicted translation start site were analyzed (in all cases the exact transcription initiation has not been experimentally determined). Figure 6B illustrates the relative position of the putative cis-regulatory elements identified by using visual inspection or the plant cis-acting regulatory DNA element database (PLACE; Higo et al. 1999). None of the *NLE* promoters analyzed have an obvious TATA box but all of them possess a putative basic promoter CAAT box. In the *ScNLE* promoter, the CAAT box is located in the –400 to –113 region, which was found to be essential for driving the expression of *GUS* in several tissues of the ovary 48 HAP (Figs. 5G–H, 6). Four sequences showing a nine in 10 match to the CArG box (consensus CC[A/T]$_6$GG), bound by MADS domain proteins (Acton et al. 1997; Huang et al. 1993), were identified in the –1,171 to –695 and –695 to –400 region of *ScNLE* promoter, which were shown to be required for fertilization-dependent response and tissue-specific repression of *GUS* expression, respectively (Figs. 5F–G, 6). The core binding sequence of the *Arabidopsis* PRHA homeodomain transcription factor (TAATTG) (Plesch et al. 1997) was additionally found in the same region. In *A. thaliana*, two putative CArG boxes and three PRHA binding sites were identified within the first 927 bp of the extended promoter. In *P. trichocarpa*, two putative CArG boxes and one PRHA binding site were found within 1,194 bp whereas in *O. sativa*, one putative CArG box and no PRHA binding site were found within 1,166 bp. Finally, several AAAG sequences, representing the core binding site of Dof transcription factors (Yanagisawa 2004), are scattered along all the *NLE* promoter sequences analyzed. In the *ScNLE* promoter, these are present in all the deletion regions analyzed. Dof transcription factors are known to interact with bZIP (Conlan et al. 1999) and MYB (Diaz et al. 2005, 2002) binding proteins. No core sequence for bZIP binding (ACGT) have been found in the 1,171 bp upstream region of *ScNLE* promoter but several sequence motifs recognized by different MYB transcription factors have been found by the PLACE database (data not shown) in the all the *NLE* promoters analyzed.

Reducing *ScNLE* expression levels in *S. chacoense* caused reduced fertility

To investigate the function of *ScNLE* during plant reproductive development, we generated transgenic *ScNLE* underexpressing lines and analyzed the phenotypes associated with ovary development following fertilization. WT *S. chacoense* plants were transformed with part of the *ScNLE* cDNA either in the antisense orientation (asNLE lines) or as a double-stranded RNA construct (iNLE lines) driven by the strong and constitutive CaMV 35S promoter. Among the transgenic lines obtained, a total of four lines, namely asNLE3, asNLE5, iNLE5, and iNLE6, showed similar pleiotropic phenotypes including dwarfism (Fig. 7A) and defects in seed and fruit development (Fig. 7E–G). RT-PCR analyses using primers that annealed to a region of *ScNLE* cDNA not included in the transgene constructs revealed that all four lines had reduced endogenous *ScNLE* transcripts in apex tissues relative to the WT (Fig. 7B). Severity of the phenotypes in these lines did not however correlate with the severity in *ScNLE* expression reduction. While asNLE5 and iNLE6 showed the strongest phenotypes and an average of 88% and 62% of WT transcript levels, respectively, the asNLE3 had intermediate phenotypes with 28% of transcripts, and iNLE5 was mildly affected in some developmental aspects despite a reduction of transcripts to 32%. This absence of correlation is consistent with results obtained in previous studies showing that the production of abnormal phenotypes induced by RNAi is not always correlated with a significant decrease in transcript levels (Acosta-Garcia and Vielle-Calzada 2004; Kerschen et al. 2004). Futhermore, the phenotypes were stably maintained over time.

In the extreme case of iNLE6 line, flower buds sometimes initiated but always dropped at very early stages of their formation. This phenomenon was also observed for the asNLE5 line with the exception that some of the buds could reach maturity. Because asNLE3 and asNLE5 showed the more obvious post-fertilization defects, phenotype analyzes were carried out in these lines. Flowers formed from these underexpressing lines produced apparently normal ovule-containing ovaries (Fig. 7C, D). However, when asNLE3 and asNLE5 flowers were cross-pollinated with WT compatible pollen, their fruits were always

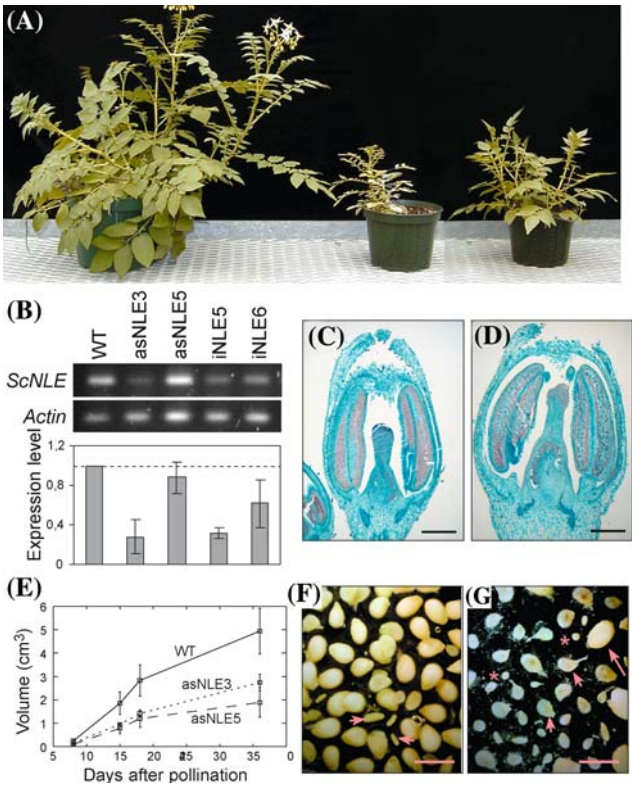

Fig. 7 Phenotypic analysis of *ScNLE* underexpressing lines. (**A**) 10-week-old WT (left), asNLE3 (middle), and asNLE5 (left) lines. Bar = 5 cm. (**B**) RT-PCR analysis of *ScNLE* mRNA expression levels in WT and *ScNLE* antisense (as) and double-stranded RNA (i) lines (top). *ACTIN* served as an internal control (middle). Relative quantification of *ScNLE* expression levels (bottom). (**C**, **D**) Longitudinal sections of representative flowers before anthesis from (**C**) WT and (**D**) asNLE5 lines. Bar = 500 μm. (**E**) Fruit growth. Fruit volumes of WT, asNLE3 and asNLE5 underexpressing lines were measured 8, 5, 18, and 36 days after pollination ($n = 10$). (**F**, **G**) Seeds isolated from fruits of (**F**) WT and (**G**) asNLE5 lines. Bar = 4 mm

smaller than those produced from WT plants during the course of their development (Fig. 7E). At maturity, at 36 DAP, sizes of asNLE3 and asNLE5 fruits were about 55% and 40%, respectively, of the WT fruits. Both asNLE3 and asNLE5 mature fruits had higher proportions of small aborted ovules and aborted seeds than the WT. More exhaustive dissection of asNLE5 mature fruits revealed 30% of small aborted ovules, 60% of flat aborted seeds of varied sizes, and 10% of bulging embryo-containing seeds (Fig. 7G). In contrast, WT seeds contained an average of 1% aborted ovules, 25% aborted seeds and 74% embryo-containing seeds (Fig. 7F). High occurrence of natural seed failure has been reported in numerous Solanaceous species (Clarke 1940; Dnyansagar and Cooper 1960; Kapil and Tiwari 1978). The high proportions of aborted ovules and seeds obtained in the asNLE5 underexpressing line suggest that *ScNLE* plays an essential role in reproductive processes in the female organs.

Discussion

Using a negative selection screen for weakly expressed mRNAs in fertilized ovaries we have isolated in the wild potato species *Solanum chacoense*, a homolog of the *Drosophila NOTCHLESS* (*NLE*) gene, which encodes a WDR protein. *DmNLE* was isolated in *Drosophila* through a genetic screen for modifiers of Notch signaling activity, and its name comes from the analysis of loss-of-function *nle* mutant alleles that dominantly suppress the wing notching caused by some Notch alleles (Royet et al. 1998). Overexpression of *NLE* in *Xenopus* and *Drosophila* also exerts a dominant-negative effect in that it also increases Notch activity. In *Drosophila*, genetic and biochemical evidences show that DmNLE modifies Notch signaling activity through a direct interaction with the Notch receptor intracellular domain (Royet et al. 1998). Although the Notch pathway does not exist in plants and yeasts, *NLE* is nonetheless highly conversed between animals, plants, and yeast, suggesting therefore functional conservation of the gene in these organisms.

In this study, we have demonstrated that the plant *ScNLE* gene can affect bristle formation similarly to *DmNLE* when overexpressed in the fruitfly (Fig. 1B–C). This finding is interesting as it requires that ScNLE is able to interact with the *Drosophila* Notch intracellular domain and possibly with other regulatory components of the pathway. Therefore, ScNLE and DmNLE are likely to share an analogous mode of action and to be part of cellular processes common to both plants, yeast, and animals. The additional and unique phenotypes produced by strong *ScNLE* overexpressing flies (Fig. 1C) could be attributed to a difference in protein–protein interaction efficiency between the plant ScNLE protein and Notch pathway components. This hypothesis is supported by the weak sequence conservation between several corresponding surface-exposed regions (regions I and II in Fig. 1A) of ScNLE and DmNLE. These regions are thought to confer specificity of interaction with protein partners and WD repeats having more similar surface-exposed regions are more likely to share common binding partners (Smith et al. 1999). Because most of the Notch pathway components do not exist in plants (and yeast), the conserved cellular function of NLE would have adapted to serve separately animal-specific and plant-specific developmental processes. Accordingly, plants and animals use divergent signaling

pathways (Wigge and Weigel 2001). With about 417 members in *Arabidopsis*, receptor-like kinases (RLKs) constitute the largest family of transmembrane receptor in higher plants (Shiu and Bleecker 2001) and therefore represent a most probable candidate if ScNLE regulates the activity of a receptor in plants. Such a situation would then be a reminder of AGB1, a WDR protein orthologous to the Gβ subunit of the heterotrimeric G protein. In animals, G protein associates with the intracellular domain of G Protein-Coupled Receptors (GPCRs). In plants, although the homolog of the Gα subunit GPA1 was reported to interact with a GPCR-type of receptor (GCR1) (Pandey and Assmann 2004), genetic evidences also suggest that AGB1 would interact with ERECTA, a leucine-rich repeat receptor-like kinase (LRR-RLK) (Lease et al. 2001).

The importance of the *NLE* gene during plant growth and development was also revealed in this study. The expression pattern of the gene and the pleiotropic phenotypes caused by its underexpression showed that *ScNLE* is used reiteratively in multiple developmental processes, which may not be surprising since WDR proteins are able to mediate interactions with multiple binding partners in a sequential and/or simultaneous manner (Smith et al. 1999).

In addition of being involved in plant vegetative development, we have shown that *ScNLE* plays other roles during fertilization and/or post-fertilization events. *ScNLE* mRNA expression was up-regulated immediately following fertilization and this increase was transient, with *ScNLE* expression going down to basal levels within 2 days after the initial up-regulation. Moreover, expression of *ScNLE* in the ovary 48 HAP showed localization in specific tissues including the placenta, the vascular tissues and the endothelial cells of ovules. We further demonstrated that underexpressing *ScNLE* led to the production of smaller fruits that contained mostly aborted ovules and aborted seeds. While these data clearly indicate a role for *ScNLE* during fertilization and/or early post-fertilization events, how the gene influences these processes still needs to be defined. In flowering plants, seeds and fruits develop from ovules and ovaries, respectively, in response to double-fertilization of the embryo sac by the two spermatic cells of a pollen (Goldberg et al. 1989). A period of intensive cell division characterizes the first stage of fruit development following fertilization (Tanksley 2004). The endothelium of ovules, which is a specialized tissue layer of the integument closest to the embryo sac, appears to perform diverse functions depending on the stage of seed development, from coordinating growth of the ovule to later feeding and protecting the developing embryo sac and embryo (Kapil and Tiwari 1978). Therefore, the transient up-regulation of *ScNLE* in the ovary could perhaps participate in a cellular process triggered by fertilization and that is essential in the initiation of seed and fruit development, such as cell proliferation. Once the program initiated, high *ScNLE* activity would be dispensable and down-regulated. Although *NLE* is likely involved in plant fertilization response, preliminary screening of *AtNLE* RNAi lines in *Arabidopsis* indicates that development of the female gametophyte is arrested after megaspore formation, suggesting that megagametogenesis could also be impaired in aborted ovules of *ScNLE* underexpressing lines (Gray-Mitsumune, M. and Matton, D. P., unpublished observation).

Similarly to *ScNLE*, several genes that have been shown to be expressed in the endothelium of ovules and other tissues of the ovary are also expressed in the shoot apex (Bowman et al. 1991; Lu et al. 1996; Porat et al. 1998). Although the overall morphology of the ovaries produced by *ScNLE* underexpressing lines looked similar to the WT, it cannot be excluded that more subtle defects in ovary formation arising from the plant apex (meristem) could contribute in part to the post-fertilization phenotypes observed in these lines. Therefore, the specific function of *ScNLE* in the ovary in response to fertilization would need to be ascertained in transgenic plants with *ScNLE* underexpression driven by an inducible promoter system or a tissue-specific promoter.

We carried a 5′ deletion analysis as a first step in trying to delineate the *cis* regions regulating the specific activity of the *ScNLE* promoter in the ovary following fertilization (48 HAP). This analysis revealed that *ScNLE* expression pattern is driven by a mosaic of positive, negative, and tissue specific regulatory elements acting through different regions of the promoter. Region –400 to –113 was found to be essential for most of the positive regulation of *ScNLE*, since its deletion completely abrogated transcription of *uidA* reporter gene in every tissues of the ovary except the placenta, in which expression seemed to be conferred by the –113 to +58 region. The –400 to –113 region was however unable to confer the tissue-specific expression pattern of endogenous *ScNLE* as determined by in situ hybridization. Instead, region –695 to –400 seemed to contain negative regulatory elements for restricting the activity of the *ScNLE* promoter in some of the determined tissues (placenta, funiculus), since its removal led to a widespread and unspecific distribution of GUS throughout the ovary. A similar active repression conferring cell-specific expression

was shown for the pollen generative cell-expressed gene *LGC1* (Singh et al. 2003). Despite the analysis of more than 1 kb of promoter region, the 1,171 bp *ScNLE* region analyzed did not completely recapitulate the expression pattern of the endogenous *ScNLE* gene as revealed by in situ hybridization, such as the presence of transcripts in the endothelium of ovules and vascular tissues of the placenta, and the absence of expression in the receptacle outside the vascular tissues. There are several explanations for such discrepancies. For example, the GUS staining in the receptacle outside the vascular tissues could have been the result of leakage of the GUS enzyme or of the X-gluc reaction product from the vascular tissues of the receptacle to surrounding tissues because of strong GUS accumulation. Moreover, the promoter region analyzed does probably not contain all the regulatory elements required for complete and proper *ScNLE* expression pattern. Although numerous examples of promoter analysis have shown that promoter regions with a size in range of several hundreds bp to 1 kb upstream of the gene reproduce faithful expression patterns of reporter genes in vivo, other studies have shown the requirement of sequences further upstream (Lee et al. 2005), downstream of the gene (Larkin et al. 1993), as well as in introns (Sieburth and Meyerowitz 1997).

Regions required for *ScNLE* promoter responsiveness to fertilization were also determined. RNA gel blot analyses carried with both isolated ovules (containing few placental tissue contamination) and whole ovaries clearly showed that endogenous *ScNLE* expression level is very weak in ovaries at 0 HAP, in absence of fertilization, but is highly increased from 36 to 48 HAP, corresponding to a period of intense fertilization in *S. chacoense*. Our *ScNLE* promoter deletion analyzes pointed to an initial active repression of *ScNLE* expression in the ovary in absence of fertilization, that is conferred by a regulatory element in the –1,171 to –695 region, since removal of this region led to considerably higher basal *GUS* expression levels in ovaries 0 HAP compared to endogenous *ScNLE*. Also, *ScNLE* responsiveness to fertilization is likely controlled by a positive regulatory element located in the –400 to –113 region of the promoter, since the presence of this region allowed an increase in *GUS* expression levels in ovaries from 0 to 48 HAP but its removal abolished such increase in fertilized ovaries. The expression of *GUS* driven by the determined regulatory regions fused to a minimal 35S promoter should confirm their respective roles in the regulation of *ScNLE* gene expression in the ovary.

We analyzed the *ScNLE* promoter sequence for regulatory motifs with the aim of correlating the identified regulatory regions to transcription factors whose expression in space and time has been shown by in situ hybridization to overlap, at least in part, with that of *ScNLE*. These transcription factors would represent candidate positive and negative regulators controlling *ScNLE* promoter activity. Several regulatory motifs were found. For example, deletion of the putative CAAT box, a basic promoter element, and of a Dof transcription factor binding site (AAAG motif) could explain the major loss of *ScNLE* promoter activity when region –400 to –113 was deleted. Since the core Dof recognition motif is short, finding numerous AAAG motifs distributed along *ScNLE* promoter is not significant by itself. The DAG1 Dof transcription factor have however been shown to be expressed in the vascular tissues of the gynoecium and in the funiculus after fertilization in *Arabidopsis* (Papi et al. 2000). Similarly, PRHA homeodomain transcription factor, for which one putative binding site was identified in *ScNLE* promoter sequence, is associated to developing vascular tissues (Plesch et al. 1997). In addition, we found four very close matches to the CArG box motif, recognized by MADS domain transcription factors (Acton et al. 1997; Huang et al. 1993), of which two are located in the –1,171 to –695 region required for most of *ScNLE* promoter responsiveness to fertilization. Interestingly, numerous MADS-box genes of tomato, a close relative of *S. chacoense*, were shown to be induced soon after fertilization in a combination of tissues in the ovary including vascular tissues, placenta, and the endothelium of ovules (Busi et al. 2003). Most of all these identified putative binding sites were also found in the putative *NLE* promoter of three other plant species. The final determination of the functions of these putative binding sites will however require site-directed mutagenesis altering these sequences to be performed.

Acknowledgements We are indebt to Dr. Stephen Cohen from the European Molecular Biology Laboratory, Heidelberg, Germany, where part of the work was realized in his laboratory on *Drosophila* transgenic experiments. We also thank Roselyne Labbé, Édtih Lafleur and Éric Chevalier for technical assistance. This work was supported by the Natural Sciences and Engineering Research Council of Canada (NSERC) and from the Canada Research Chair program. S. C. Chantha is the recipient of Ph.D. fellowships from NSERC and from Le Fonds Québécois de la Recherche sur la Nature et les Technologies (FQRNT, Québec). D. P. Matton holds a Canada Research Chair in Functional Genomics and Plant Signal Transduction.

References

Acosta-Garcia G, Vielle-Calzada JP (2004) A classical arabinogalactan protein is essential for the initiation of female gametogenesis in *Arabidopsis*. Plant Cell 16:2614–2628

Acton TB, Zhong H, Vershon AK (1997) DNA-binding specificity of Mcm1: operator mutations that alter DNA-binding and transcriptional activities by a MADS box protein. Mol Cell Biol 17:1881–1889

Artavanis-Tsakonas S, Rand MD, Lake RJ (1999) Notch signaling: cell fate control and signal integration in development. Science 284:770–776

Bowman JL, Drews GN, Meyerowitz EM (1991) Expression of the *Arabidopsis* floral homeotic gene AGAMOUS is restricted to specific cell types late in flower development. Plant Cell 3:749–758

Busi MV, Bustamante C, D'angelo C, Hidalgo-Cuevas M, Boggio SB, Valle EM, Zabaleta E (2003) MADS-box genes expressed during tomato seed and fruit development. Plant Mol Biol 52:801–815

Bussiere F, Ledu S, Girard M, Heroux M, Perreault J-P, Matton DP (2003) Development of an efficient cis-trans-cis ribozyme cassette to inactivate plant genes. Plant Biotechnol J 1:423–435

Cebolla A, Vinardell JM, Kiss E, Olah B, Roudier F, Kondorosi A, Kondorosi E (1999) The mitotic inhibitor ccs52 is required for endoreduplication and ploidy-dependent cell enlargement in plants. Embo J 18:4476–4484

Chaudhury AM, Ming L, Miller C, Craig S, Dennis ES, Peacock WJ (1997) Fertilization-independent seed development in *Arabidopsis thaliana*. Proc Natl Acad Sci USA 94:4223–4228

Clarke AE (1940) Fertilization and early embryo development in the potato. Am Potato J 17:20–25

Conlan RS, Hammond-Kosack M, Bevan M (1999) Transcription activation mediated by the bZIP factor SPA on the endosperm box is modulated by ESBF-1 in vitro. Plant J 19:173–181

Conner J, Liu Z (2000) LEUNIG, a putative transcriptional corepressor that regulates AGAMOUS expression during flower development. Proc Natl Acad Sci USA 97:12902–12907

Deng XW, Caspar T, Quail PH (1991) cop1: a regulatory locus involved in light-controlled development and gene expression in *Arabidopsis*. Genes Dev 5:1172–1182

Diaz I, Martinez M, Isabel-Lamoneda I, Rubio-Somoza I, Carbonero P (2005) The DOF protein, SAD, interacts with GAMYB in plant nuclei and activates transcription of endosperm-specific genes during barley seed development. Plant J 42:652–662

Diaz I, Vicente-Carbajosa J, Abraham Z, Martinez M, Isabel-La Moneda I, Carbonero P (2002) The GAMYB protein from barley interacts with the DOF transcription factor BPBF and activates endosperm-specific genes during seed development. Plant J 29:453–464

Dnyansagar VR, Cooper DC (1960) Development of the seed of *Solanum phureja*. Am J Bot 47:176–186

Germain H, Rudd S, Zotti C, Caron S, O'brien M, Chantha SC, Lagace M, Major F, Matton DP (2005) A 6374 unigene set corresponding to low abundance transcripts expressed following fertilization in *Solanum chacoense* Bitt, and characterization of 30 receptor-like kinases. Plant Mol Biol 59:515–532

Gillaspy G, Ben-David H, Gruissem W (1993) Fruits: a developmental perspective. Plant Cell 5:1439–1451

Goldberg RB, Barker SJ, Perez-Grau L (1989) Regulation of gene expression during plant embryogenesis. Cell 56:149–160

Guitton AE, Berger F (2005) Loss of function of MULTICOPY SUPPRESSOR OF IRA 1 produces nonviable parthenogenetic embryos in *Arabidopsis*. Curr Biol 15:750–754

Higo K, Ugawa Y, Iwamoto M, Korenaga T (1999) Plant cis-acting regulatory DNA elements (PLACE) database: 1999. Nucleic Acids Res 27:297–300

Honma T, Goto K (2000) The *Arabidopsis* floral homeotic gene PISTILLATA is regulated by discrete cis-elements responsive to induction and maintenance signals. Development 127:2021–2030

Hu W, Wang Y, Bowers C, Ma H (2003) Isolation, sequence analysis, and expression studies of florally expressed cDNAs in *Arabidopsis*. Plant Mol Biol 53:545–563

Huang H, Mizukami Y, Hu Y, Ma H (1993) Isolation and characterization of the binding sequences for the product of the *Arabidopsis* floral homeotic gene AGAMOUS. Nucleic Acids Res 21:4769–4776

Huck N, Moore JM, Federer M, Grossniklaus U (2003) The *Arabidopsis* mutant feronia disrupts the female gametophytic control of pollen tube reception. Development 130:2149–2159

Joshi CP, Zhou H, Huang X, Chiang VL (1997) Context sequences of translation initiation codon in plants. Plant Mol Biol 35:993–1001

Kadesch T (2000) Notch signaling: a dance of proteins changing partners. Exp Cell Res 260:1–8

Kapil RN, Tiwari SC (1978) The integumentary tapetum. Bot Rev 44:457–490

Kerschen A, Napoli CA, Jorgensen RA, Muller AE (2004) Effectiveness of RNA interference in transgenic plants. FEBS Lett 566:223–228

Kim MK, Choi JW, Jeon JH, Franceschi VR, Davin LB, Lewis NG (2002) Specimen block counter-staining for localization of GUS expression in transgenic arabidopsis and tobacco. Plant Cell Rep 21:35–39

Kimble J, Simpson P (1997) The LIN-12/Notch signaling pathway and its regulation. Annu Rev Cell Dev Biol 13:333–361

Kohler C, Hennig L, Bouveret R, Gheyselinck J, Grossniklaus U, Gruissem W (2003) *Arabidopsis* MSI1 is a component of the MEA/FIE Polycomb group complex and required for seed development. Embo J 22:4804–4814

Lagacé M, Chantha SC, Major G, Matton DP (2003) Fertilization induces strong accumulation of a histone deacetylase (HD2) and of other chromatin-remodeling proteins in restricted areas of the ovules. Plant Mol Biol 53:759–769

Lantin S, O'brien M, Matton DP (1999) Pollination, wounding and jasmonate treatments induce the expression of a developmentally regulated pistil dioxygenase at a distance, in the ovary, in the wild potato *Solanum chacoense* Bitt. Plant Mol Biol 41:371–386

Larkin JC, Oppenheimer DG, Pollock S, Marks MD (1993) *Arabidopsis* GLABROUS1 gene requires downstream sequences for function. Plant Cell 5:1739–1748

Le Bras S, Cohen-Tannoudji M, Guyot V, Vandormael-Pournin S, Coumailleau F, Babinet C, Baldacci P (2002) Transcript map of the Ovum mutant (Om) locus: isolation by exon trapping of new candidate genes for the DDK syndrome. Gene 296:75–86

Lease KA, Wen J, Li J, Doke JT, Liscum E, Walker JC (2001) A mutant *Arabidopsis* heterotrimeric G-protein beta subunit affects leaf, flower, and fruit development. Plant Cell 13:2631–2641

Lee JY, Baum SF, Alvarez J, Patel A, Chitwood DH, Bowman JL (2005) Activation of CRABS CLAW in the Nectaries and Carpels of *Arabidopsis*. Plant Cell 17:25–36

Lu P, Porat R, Nadeau JA, O'neill SD (1996) Identification of a meristem L1 layer-specific gene in *Arabidopsis* that is expressed during embryonic pattern formation and defines a new class of homeobox genes. Plant Cell 8:2155–2168

Marton ML, Cordts S, Broadhvest J, Dresselhaus T (2005) Micropylar pollen tube guidance by egg apparatus 1 of maize. Science 307:573–576

Matton DP, Maes O, Laublin G, Xike Q, Bertrand C, Morse D, Cappadocia M (1997) Hypervariable domains of self-incompatibility RNases mediate allele-specific pollen recognition. Plant Cell 9:1757–1766

Neer EJ, Schmidt CJ, Nambudripad R, Smith TF (1994) The ancient regulatory-protein family of WD-repeat proteins. Nature 371:297–300

O'Brien M, Kapfer C, Major G, Laurin M, Bertrand C, Kondo K, Kowyama Y, Matton DP (2002) Molecular analysis of the stylar-expressed *Solanum chacoense* small asparagine-rich protein family related to the HT modifier of gametophytic self-incompatibility in *Nicotiana*. Plant J 32:985–996

Ohad N, Margossian L, Hsu YC, Williams C, Repetti P, Fischer RL (1996) A mutation that allows endosperm development without fertilization. Proc Natl Acad Sci USA 93:5319–5324

Osterlund MT, Hardtke CS, Wei N, Deng XW (2000) Targeted destabilization of HY5 during light-regulated development of *Arabidopsis*. Nature 405:462–466

Pandey S, Assmann SM (2004) The *Arabidopsis* putative G protein-coupled receptor GCR1 interacts with the G protein alpha subunit GPA1 and regulates abscisic acid signaling. Plant Cell 16:1616–1632

Papi M, Sabatini S, Bouchez D, Camilleri C, Costantino P, Vittorioso P (2000) Identification and disruption of an *Arabidopsis* zinc finger gene controlling seed germination. Genes Dev 14:28–33

Plesch G, Stormann K, Torres JT, Walden R, Somssich IE (1997) Developmental and auxin-induced expression of the *Arabidopsis* prha homeobox gene. Plant J 12:635–647

Porat R, Lu P, O'neill SD (1998) *Arabidopsis* SKP1, a homologue of a cell cycle regulator gene, is predominantly expressed in meristematic cells. Planta 204:345–351

Rotman N, Rozier F, Boavida L, Dumas C, Berger F, Faure JE (2003) Female control of male gamete delivery during fertilization in *Arabidopsis thaliana*. Curr Biol 13:432–436

Royet J, Bouwmeester T, Cohen SM (1998) Notchless encodes a novel WD40-repeat-containing protein that modulates Notch signaling activity. Embo J 17:7351–7360

Shiu SH, Bleecker AB (2001) Receptor-like kinases from *Arabidopsis* form a monophyletic gene family related to animal receptor kinases. Proc Natl Acad Sci USA 98:10763–10768

Sieburth LE, Meyerowitz EM (1997) Molecular dissection of the AGAMOUS control region shows that cis elements for spatial regulation are located intragenically. Plant Cell 9:355–365

Singh M, Bhalla PL, Xu H, Singh MB (2003) Isolation and characterization of a flowering plant male gametic cell-specific promoter. FEBS Lett 542:47–52

Smith TF, Gaitatzes C, Saxena K, Neer EJ (1999) The WD repeat: a common architecture for diverse functions. Trends Biochem Sci 24:181–185

Tanksley SD (2004) The genetic, developmental, and molecular bases of fruit size and shape variation in tomato. Plant Cell 16(Suppl):S181–189

Tilly JJ, Allen DW, Jack T (1998) The CArG boxes in the promoter of the *Arabidopsis* floral organ identity gene APETALA3 mediate diverse regulatory effects. Development 125:1647–1657

Van Nocker S, Ludwig P (2003) The WD-repeat protein superfamily in *Arabidopsis*: conservation and divergence in structure and function. BMC Genom 4:50

Wigge PA, Weigel D (2001) *Arabidopsis* genome: life without notch. Curr Biol 11:R112–114

Williams EJ (1955) Seed failure in the Chippewa variety of *Solanum tuberosum*. Bot Gaz 10:10–15

Yamagishi K, Nagata N, Yee KM, Braybrook SA, Pelletier J, Fujioka S, Yoshida S, Fischer RL, Goldberg RB, Harada JJ (2005) TANMEI/EMB2757 encodes a WD repeat protein required for embryo development in *Arabidopsis*. Plant Physiol 139:163–173

Yanagisawa S (2004) Dof domain proteins: plant-specific transcription factors associated with diverse phenomena unique to plants. Plant Cell Physiol 45:386–391

Yu L, Gaitatzes C, Neer E, Smith TF (2000) Thirty-plus functional families from a single motif. Protein Sci 9:2470–2476